Parasites & Vectors

RESEARCH Open Access

Metabolomic signature of mouse cerebral cortex following *Toxoplasma gondii* infection

Jun Ma[1], Jun-Jun He[1], Jun-Ling Hou[1], Chun-Xue Zhou[2], Fu-Kai Zhang[1], Hany M. Elsheikha[3*] and Xing-Quan Zhu[1*]

Abstract

Background: The protozoan parasite *Toxoplasma gondii* infects and alters the neurotransmission in cerebral cortex and other brain regions, leading to neurobehavioral and neuropathologic changes in humans and animals. However, the molecules that contribute to these changes remain largely unknown.

Methods: We have investigated the impact of *T. gondii* infection on the overall metabolism of mouse cerebral cortex. Mass-spectrometry-based metabolomics and multivariate statistical analysis were employed to discover metabolomic signatures that discriminate between cerebral cortex of *T. gondii*-infected and uninfected control mice.

Results: Our results identified 73, 67 and 276 differentially abundant metabolites, which were involved in 25, 37 and 64 pathways at 7, 14 and 21 days post-infection (dpi), respectively. Metabolites in the unsaturated fatty acid biosynthesis pathway were upregulated as the infection progressed, indicating that *T. gondii* induces the biosynthesis of unsaturated fatty acids to promote its own growth and survival. Some of the downregulated metabolites were related to pathways, such as steroid hormone biosynthesis and arachidonic acid metabolism. Nine metabolites were identified as *T. gondii* responsive metabolites, namely galactosylsphingosine, arachidonic acid, LysoSM(d18:1), L-palmitoylcarnitine, calcitetrol, 27-Deoxy-5b-cyprinol, L-homophenylalanine, oleic acid and ceramide (d18:1/16:0).

Conclusions: Our data provide novel insight into the dysregulation of the metabolism of the mouse cerebral cortex during *T. gondii* infection and have important implications for studies of *T. gondii* pathogenesis.

Keywords: Metabolomics, Neuropathy, Cerebral cortex, *Toxoplasma gondii*, Host-parasite interaction, Metabolism

Background

Toxoplasma gondii is a worldwide prevalent pathogen with global seropositivity rates that range from 0 to over 90% [1]. *Toxoplasma gondii* has an indirect, multistage life-cycle that involves tachyzoites, bradyzoites-containing cysts and oocysts. This parasite has an exceptionally wide range of intermediate hosts including almost all warm-blooded vertebrate animals and humans. Tachyzoites and bradyzoites occur in the tissues of the intermediate hosts. However, members of the family Felidae are the only animals that can serve as the definitive host of *T. gondii*, where gametogony occurs in their intestine, resulting in the formation and excretion of oocysts in the feces. Ingestion of infectious oocysts with contaminated food or water, or eating improperly cooked or raw meat containing tissue cysts are the two main routes of *T. gondii* infection in humans.

Toxoplasma gondii establishes a quiescent infection with little to no clinical disease in most immunocompetent individuals. However, this parasite is responsible for a range of devastating sequelae in immunocompromised patients and in developing fetuses if their mothers acquire infection during pregnancy [2, 3]. In recent years, the impact of *T. gondii* infection on brain neurochemistry and the subsequent neuropsychiatric consequences

*Correspondence: hany.elsheikha@nottingham.ac.uk; xingquanzhu1@hotmail.com
[1] State Key Laboratory of Veterinary Etiological Biology, Key Laboratory of Veterinary Parasitology of Gansu Province, Lanzhou Veterinary Research Institute, Chinese Academy of Agricultural Sciences, Lanzhou 730046, Gansu, People's Republic of China
[3] Faculty of Medicine and Health Sciences, School of Veterinary Medicine and Science, University of Nottingham, Sutton Bonington Campus, Loughborough LE12 5RD, UK
Full list of author information is available at the end of the article

has received significant attention [4, 5]. Additionally, behavioral abnormalities have been observed in murine hosts in association with *T. gondii* infection [6, 7]. Disruption of glutamate metabolism, and glutamatergic and GABAergic signaling pathways in the brain are some of the mechanisms used by *T. gondii* to alter the behavior of infected hosts [5, 8]. *Toxoplasma gondii* parasites can also alter the regulation of other neuroactive substances, such as dopamine [9], quinolinic acid [10] and kynurenine [11].

Previous transcriptomics [12–14] and proteomics [15–17] studies have revealed some mechanisms by which *T. gondii* can alter gene expression and protein abundance in the brain of the affected hosts. Additionally, liquid chromatography–mass spectrometry (LC–MS)-based metabolomics analysis revealed altered metabolism of key molecules and regulatory pathways in the brain, spleen, liver, and serum of mice following *T. gondii* infection [18–21]. Given the complexity of brain structure and the wide spectrum of the neuropathological changes associated with *T. gondii* infection, it is of great interest to determine specific metabolic signature associated with *T. gondii*, particularly in key brain regions such as the cerebral cortex where *T. gondii* cysts are often found [22, 23].

Here, a LC–MS-based metabolomics approach was used to analyze the global metabolic alterations induced in the cerebral cortex of mice following *T. gondii* infection. Our findings reinforce previous findings [21] and provide new insights into *T. gondii* neuro-pathogenesis.

Methods

Animal infection and cerebral cortex collection

Mice were infected with *T. gondii* PRU strain (genotype II) to produce tissue cysts that were subsequently used for the infection experiments. A total of 36 female BALB/C mice, 3-weeks old, were purchased from Lanzhou University Laboratory Animal Center (Lanzhou, China). Mice were allocated into six groups with 6 mice per group: 7T (infected group at 7 dpi); 7C (control group at 7 dpi); 14T (infected group at 14 dpi); 14C (control group at 14 dpi); 21T (infected group at 21 dpi); and 21C (control group at 21 dpi). The mice in infected groups were challenged by oral gavage with 10 cysts of *T. gondii* PRU strain suspended in 0.5 ml PBS, whereas mice in the control groups were mock-treated with an equal volume of PBS only. All mice were provided non-medicated feed and water ad libitum throughout the experiment. At 7, 14 and 21 dpi, mice from each sampling time were humanely sacrificed by CO_2 asphyxiation. Cerebral cortex of each mouse was dissected with scissors and forceps, and washed immediately with PBS to remove the blood. The isolated cerebral cortices were stored frozen at − 80 °C until use.

Detection of *T. gondii* infection in the cerebral cortex of mice

Equal parts of the collected cerebral cortices were used for DNA extraction. DNA of each cerebral cortex sample was extracted using a TIANamp Genomic DNA kit (TianGen, Beijing, China) according to the manufacturer's instructions. *Toxoplasma gondii* infection was detected by PCR using primers that target the *B1* gene (F: 5′-TGC ATA GGT TGC AGT CAC TG-3′ and R: 5′-TCT TTA AAG CGT TCG TGG TC-3′). The amplification conditions were: 95 °C for 5 min followed by 35 cycles of 95 °C for 10 s, 60 °C for 10 s and 72 °C for 20 s. A negative control template (PBS) was included in each PCR run to exclude the false positive results. Positive amplified fragments were submitted to the Genewiz company (Beijing, China) for sequencing in both directions.

Metabolite extraction

The frozen cerebral cortices were taken out of the − 80 °C freezer and kept at − 20 °C for 30 min, and then at 4 °C to defrost gradually. Approximately 25 mg of each defrosted tissue sample were used for metabolite extraction by mixing with 800 µl of H_2O/MeOH (50:50% v/v) and lysis using TissueLyse bead-mill homogenizer (Qiagen, Hilden, Germany). The cerebral cortex homogenates were centrifuged at 25,000×*g* for 20 min at 4 °C. Supernatants were transferred into new tubes and 50 µl of each supernatant were filtered using a SPE column (Strata TM-X 33 µm polymeric reversed phase column, Phenomenex, Torrance, CA, USA) for solid phase extraction, and the soluble metabolites were dissolved in acetonitrile. Approximately 20 µl from each sample were pooled together as a QC sample and used to assess the reproducibility and reliability of the LC–MS method. The extracted metabolites were stored at − 80 °C until use.

LC–MS/MS analysis

The soluble metabolomics (including hydrophobic molecules) of all samples were analyzed. All chromatographic separations were performed using an ultra-performance liquid chromatography (UPLC) system (Waters, Manchester, UK). An ACQUITY UPLC BEH C18 column (100 × 2.1 mm, 1.7 µm; Waters) was used for the reversed phase separation. The column oven was maintained at 50 °C. The flow rate was set at 0.4 ml/min and the mobile phase consisted of solvent A (water + 0.1% formic acid) and solvent B (acetonitrile + 0.1% formic acid). A gradient elution process was performed to elute metabolites as follows: 100% solvent A (water + 0.1% formic acid) for

0–2 min; 0–100% solvent B (acetonitrile + 0.1% formic acid) for ~ 11 min; 100% solvent B for 11–13 min; 100% solvent A for 13–15 min. The eluted metabolites were analyzed using a high-resolution tandem mass spectrometer, SYNAPT G2 XS QTOF (Waters). For both positive and negative ion modes, the capillary and sampling cone voltages were set at 2 kV and 40 V, respectively. The TOF mass range ranged from 50 to 1200 Da and the scan time was 0.2 s. For the MS/MS detection, all precursors were fragmented using 20–40 eV, and the scan time was 0.2 s. During the acquisition, the LE signal was acquired every 3 s to calibrate the mass accuracy. Centroid MSE (mean square error) mode was used for the collection of mass spectrometry data.

Metabolite identification and multivariate statistical analysis

The raw data were imported into the software Progenesis QI v. 2.2 for peak detection and alignment. The assigned modified metabolites were identified by searching the HMDB database (http://www.hmdb.ca/spectra/ms/search) using Progenesis QI. The molecular mass data (m/z) and retention time (min) were used to identify the metabolites. The putative metabolites were mapped to the Kyoto Encyclopedia of Genes and Genomes (KEGG; http://www.genome.jp/kegg/) by matching the *m*/*z* of our samples with those from the database. The pre-processed data were imported to *metaX*, a R package software for statistical analysis. Student's *t*-test was used to identify significantly different metabolites between infected and control mouse groups, and $P < 0.05$ was considered significant. *P*-values were adjusted for multiple testing using the Benjamini–Hochberg method at a false discovery rate threshold of 5%. The dataset was also subjected to unsupervised multivariate statistical analyses, including principal component analysis (PCA) and partial least-square discriminant analysis (PLS-DA), using SIMCA v.13.0 software. *Toxoplasma gondii* responsive metabolites were identified using receiver-operating characteristic (ROC) curve analysis by calculating the area under the curve (AUC) using the *pROC* package in R. Cytoscape v.3.3 was used for visualization of relationship among metabolites and pathways.

Results

Confirmation of infection

PCR coupled with sequencing analysis confirmed that all cerebral cortices collected from infected mice at 7, 14 and 21 dpi were *T. gondii* B1 gene positive (Additional file 1: Figure S1). No positive amplification products of *T. gondii* B1 gene were detected in cerebral cortices of mice in the control groups (Additional file 1: Figure S1). At 14 dpi, mice in infected groups showed clinical signs such as anorexia, hunched back and ruffled fur. None of these clinical signs were observed in the control mice at 14 dpi. At 21 dpi, mice in infected group seemed to regain their normal physical status.

Infection-related metabolic changes

A total of 3200 ions were detected in the negative electrospray ionization (ESI−) mode and 1436 metabolites were putatively identified, whereas 6198 ions were detected in the positive electrospray ionization (ESI+) mode with 3952 metabolites putatively identified. PLS-DA analysis was performed to identify the differences in the metabolic profile between infected and non-infected cerebral cortices. As shown in Fig. 1, in both positive and negative ion modes, the metabolites of infected and control cerebral cortices were clustered in separate groups. Additionally, as the infection developed at 14 and 21 dpi, the differences and separation between infected and non-infected cerebral cortices increased. This result indicates that the metabolic patterns of the infected cerebral cortices are distinct from those of non-infected cerebral cortices.

Time-dependent variation in the differentially abundant metabolites

To identify the temporal differences between infected and non-infected cerebral cortices, the differences in the metabolites between *T. gondii*-infected groups and non-infected groups were analyzed at 7, 14 and 21 dpi. Dozens of differentially abundant metabolites exhibited altered levels in *T. gondii*-infected cerebral cortices. In the negative ionization mode, 64, 48 and 288 metabolites showed differential abundances at 7, 14 and 21 dpi, respectively. Furthermore, 68, 54 and 229 metabolites were differentially abundant in the positive ionization mode. The volcano and heat map plots of these metabolites are shown in Fig. 2. The details of the differentially abundant metabolites that were mapped to KEGG pathways are shown in Additional file 2: Table S1. Our analysis revealed that 22, 21 and 92 differentially abundant metabolites were mapped to KEGG pathways at 7, 14 and 21 dpi, respectively. Additionally, only 20, 10 and 80 differentially abundant metabolites were identified at 7, 14 and 21 dpi, respectively (Fig. 3a). 1-Acyl-sn-glycero-3-phosphocholine was the only differentially abundant metabolite that was altered at all three time points, where it was upregulated at 7 and 14 dpi, and downregulated at 21 dpi (Additional file 2: Table S1).

Metabolic pathways affected by *T. gondii*

As shown in Fig. 3b, the differentially abundant metabolites were involved in 25, 37 and 64 pathways, of which 6, 5 and 25 were unique at 7, 14 and 21 dpi, respectively. Twelve pathways were altered at all three sampling time points, namely metabolic pathways, biosynthesis of

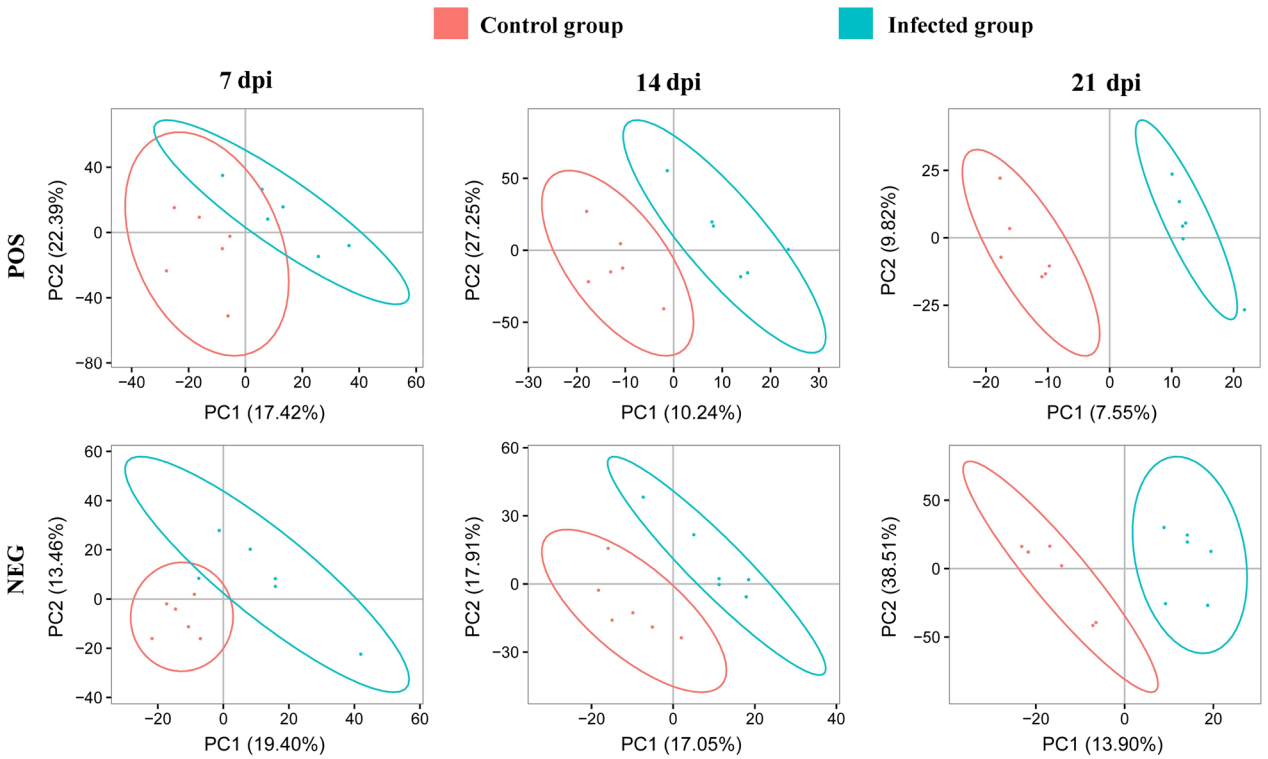

Fig. 1 Unsupervised multivariate analysis of the global metabolic changes in the cerebral cortices of mice. Partial least squares projection to latent structures discriminant analysis (PLS-DA) score plots of the first two principal components (PC1 and PC2) showing the effect of infection on the metabolic profile of cerebral cortices at 7, 14 and 21 days post-infection (dpi). Distinct metabolic differences were observed between infected and control mouse groups particularly at 14 and 21 dpi. POS and NEG indicate positive ion mode and negative ion mode, respectively

unsaturated fatty acids, glycerophospholipid metabolism, choline metabolism in cancer, regulation of autophagy, retrograde endocannabinoid signaling, primary bile acid biosynthesis, steroid hormone biosynthesis, arachidonic acid (AA) metabolism, linoleic acid metabolism, steroid biosynthesis and glycosylphosphatidylinositol (GPI)-anchor biosynthesis. Metabolites in the biosynthesis of unsaturated fatty acids pathway was upregulated as the infection progresses (Fig. 4). Metabolites in six pathways were downregulated at 21 dpi (Table 1 and Fig. 5).

Identification of *T. gondii* responsive metabolites

The results of ROC curve analysis revealed nine differentially abundant metabolites that had an AUC value > 0.8 and these were identified as *T. gondii* responsive metabolites: galactosylsphingosine, AA, LysoSM(d18:1), L-palmitoylcarnitine, calcitetrol, 27-Deoxy-5b-cyprinol, L-homophenylalanine, oleic acid and ceramide (d18:1/16:0) (Fig. 6). Among these, LysoSM (d18:1) was upregulated at 14 dpi; five metabolites (galactosylsphingosine, AA, L-palmitoylcarnitine, calcitetrol and 27-Deoxy-5b-cyprinol) exhibited differential abundance at 14 and 21 dpi, while the remaining three responsive metabolites [L-homophenylalanine, oleic acid and ceramide (d18:1/16:0)] showed differential abundance at 21 dpi. All these *T. gondii* responsive metabolites were upregulated (Additional file 2: Table S1).

Discussion

Previous research studies have indicated that *T. gondii* can alter host behavior through manipulation of signaling pathways in the brain [22, 24]. However, the metabolic

(See figure on next page.)

Fig. 2 Metabolic differences in infected cerebral cortices at 7, 14 and 21 dpi. **a** Volcano plots of the differentially abundant metabolites. The $\log_2$ fold change is shown on the x-axis. Statistical significance displayed by −log10 (*P*-value) is shown from 0 to 4 on the y-axis. Metabolites having a fold change of > 1.5 and $P < 0.05$ (Student's *t*-test) are represented by red dots. Metabolites that were not significantly changed are denoted by blue dots. Fold changes of the infected samples relative to the untreated control are based on the mean values of six biological replicates per group. **b** Heatmaps showing significantly dysregulated metabolites in the mouse cerebral cortex. Upregulated (red) or downregulated (green) metabolites (fold change > 1.5; $P < 0.5$) are indicated. POS and NEG indicate positive ion mode and negative ion mode, respectively

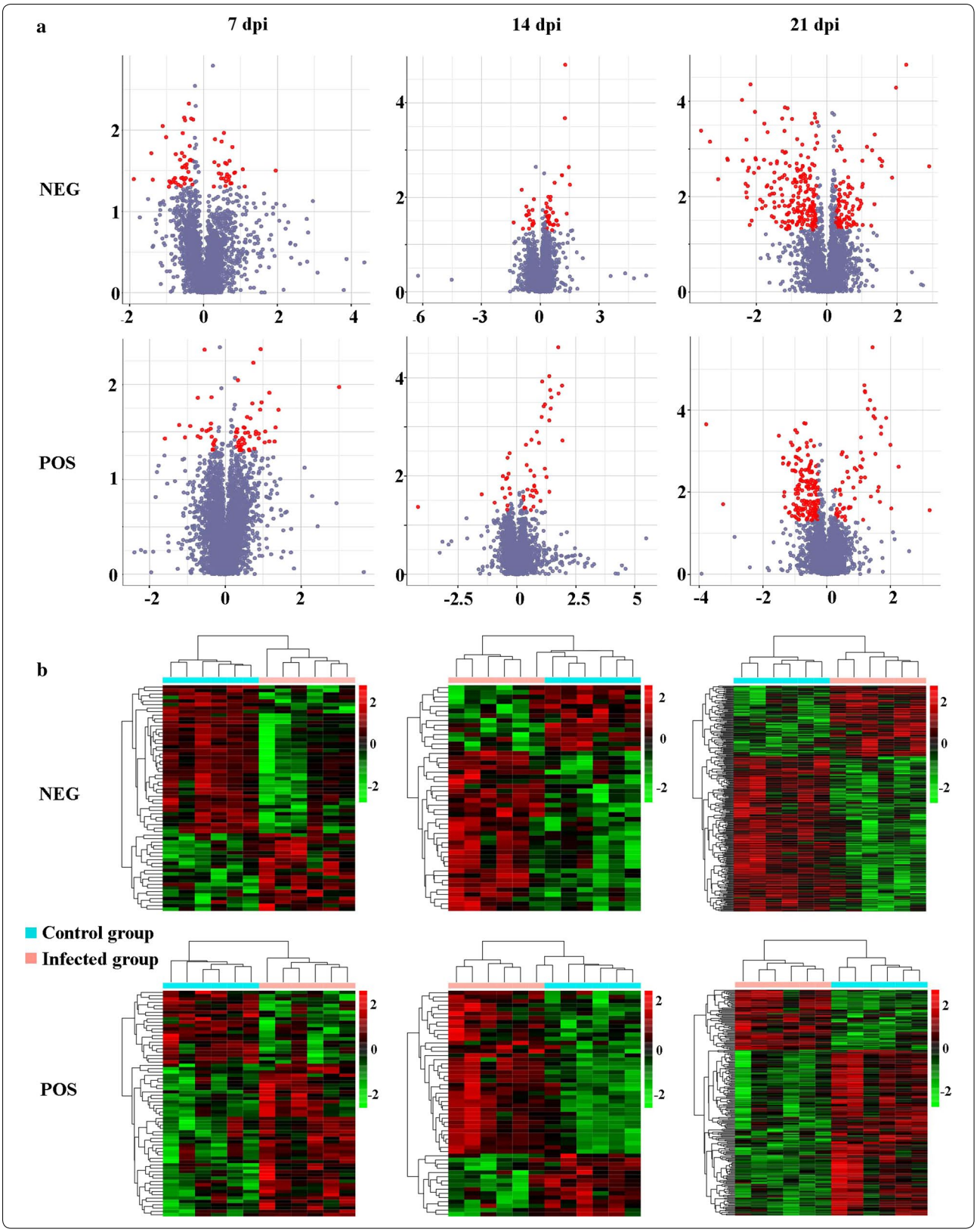
a
7 dpi
14 dpi
21 dpi
NEG
POS
b
NEG
POS
Control group
Infected group

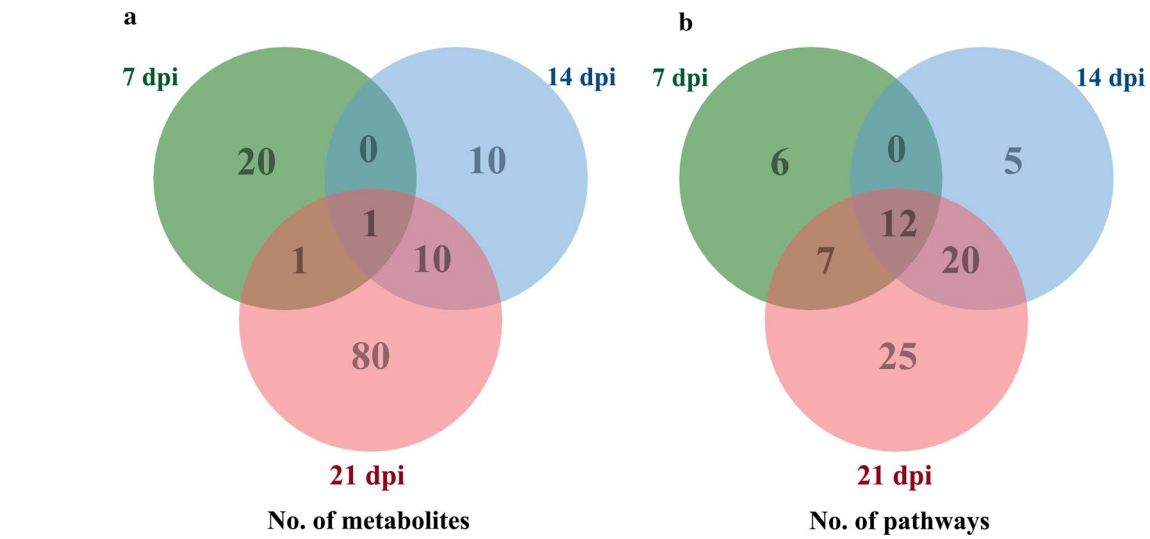

Fig. 3 Venn diagrams showing the number of **a** common and unique differentially abundant metabolites between mouse groups and **b** metabolic pathways significantly affected following infection with *T. gondii* at 7, 14 and 21 dpi

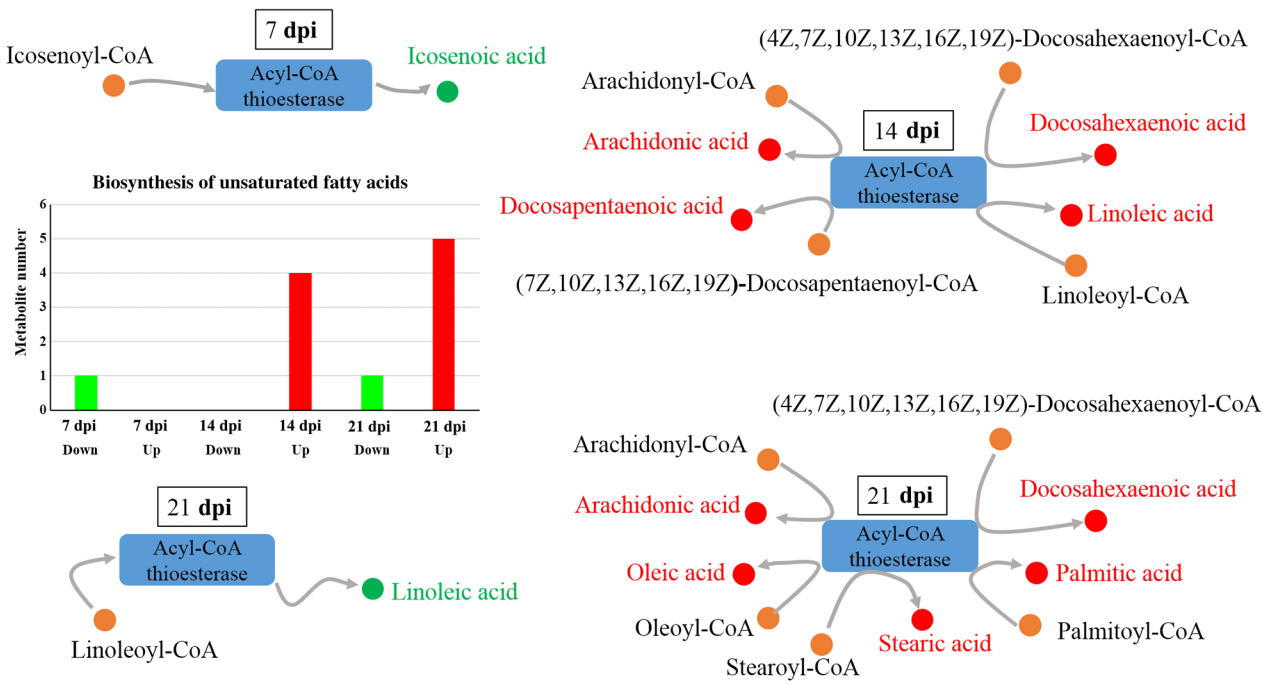

Fig. 4 Differential regulation of the metabolites involved in the biosynthesis of unsaturated fatty acids pathway at 7, 14 and 21 dpi. Red and green colors represent upregulated and downregulated metabolites, respectively

pathways involved in this process are only partially understood. Given that dysfunction of cerebral cortex underpins the neurological changes seen during *T. gondii* infection [25], the present study was set to characterize the metabolic changes of mouse cerebral cortex following *T. gondii* infection using a LC-MS-based metabolomics approach.

Metabolic changes in cerebral cortex following *T. gondii* infection

The metabolic profiles of infected cerebral cortices were different from non-infected cerebral cortices. PLS-DA analysis revealed that metabolic differences between mouse groups became more evident as the infection

Table 1 Metabolic pathways involving differentially abundant metabolites in mouse cerebral cortex at 7, 14 and 21 days after *T. gondii* infection

Pathway	7 dpi		14 dpi		21 dpi	
	Down	Up	Down	Up	Down	Up
Glycerophospholipid metabolism	0	6	3	2	21	12
Choline metabolism in cancer	0	3	0	2	14	3
Steroid hormone biosynthesis	0	1	0	2	8	2
Arachidonic acid metabolism	0	2	0	1	11	4
Linoleic acid metabolism	0	2	0	2	10	4
Steroid biosynthesis	0	1	1	1	5	2

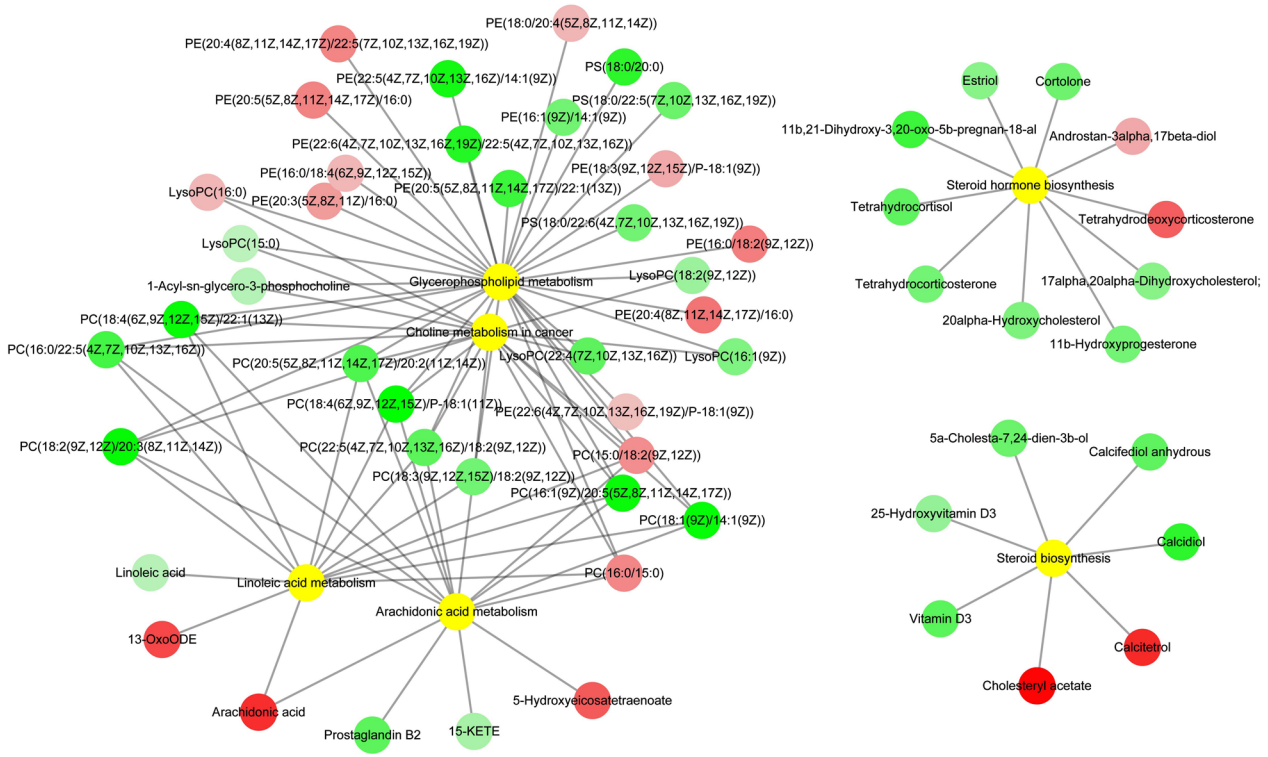

Fig. 5 Metabolic pathways associated with downregulated metabolites at 21 dpi. Red, green and yellow colors represent upregulated metabolites, downregulated metabolites and the related metabolic pathways, respectively. *Abbreviations*: PS, phosphatidylserine; PC, phosphatidylcholine; PE, phosphatidylethanolamine; 13-OxoODE, (9Z,11E)-13-oxooctadeca-9,11-dienoic acid; 15-KETE, (5Z,8Z,11Z,13E)-15-oxoicosa-5,8,11,13-tetraenoic acid

progressed from 7 to 14 and 21 dpi. In the negative ionization mode, 64, 48 and 288 metabolites were differentially abundant at 7, 14 and 21 dpi, respectively. Additionally, 68, 54 and 229 differentially abundant metabolites were detected in the positive ionization mode. Although many differentially abundant metabolites were observed in the present study, only 22, 21 and 92 differentially abundant metabolites were mapped to metabolic pathways in the KEGG database at 7, 14 and 21 dpi, respectively (Fig. 3a). The differentially abundant metabolites were involved in 25, 37 and 64 pathways at 7, 14 and 21 dpi, respectively (Fig. 3b). Although only one common differentially expressed metabolite was found at all sampling times (Fig. 3a), 12 pathways were commonly altered in all collected cerebral cortices at all time points after infection (Fig. 3b).

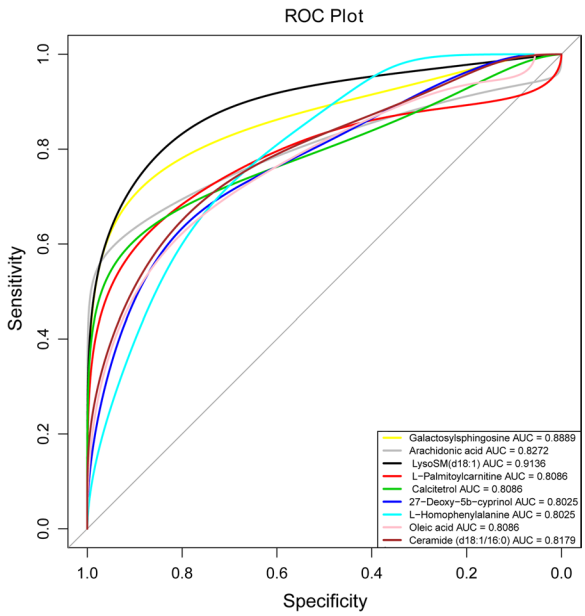

Fig. 6 Receiver operating characteristic (ROC) curve showing *T. gondii* responsive metabolites. The x- and y-axes show false positive rate and true positive rate, respectively. *Abbreviation*: AUC, area under the curve

Time-dependent increase in the upregulated metabolites

Lipids play essential roles in the pathogenesis of *T. gondii* infection; parasite replication can be limited by fatty acid biosynthesis and availability [26]. Some fatty acid biosynthesis systems exist in the apicoplast and endoplasmic reticulum of *T. gondii* [27]. *Toxoplasma gondii* also requires acquisition of certain fatty acids from host cells. The host mitochondrial fusion can restrict *T. gondii* growth by limiting the uptake of fatty acids from the host cell [28]. In our study, the metabolites associated with biosynthesis of unsaturated fatty acid pathway were upregulated in the infected samples. Previous studies showed that N-3 polyunsaturated fatty acids and monounsaturated fatty acids reduce tissue responsiveness to cytokines, whereas n-6 polyunsaturated fatty acids [29] and saturated fatty acids [30] enhance the tissue inflammatory response. Given the inflammatory role of AA [31]; the immune-regulatory activity of linoleic acid [32]; the ability of stearic acid and palmitic acid to enhance the nuclear translocation of NF-κB p65 and induction of proinflammatory response [33]; the anti-inflammatory activity of docosahexaenoic acid in humans [34]; the synergistic effect of docosapentaenoic acid on the anti-inflammatory function of docosahexaenoic acid [35]; and the inversely proportional relationship of oleic acid with natural killer cell activity [36], which is essential for *T. gondii* eradication [35], it is tempting to speculate that unsaturated fatty acids contribute to the regulation of host immune responses to *T. gondii* infection.

Noteworthy in our study is the upregulation of the immune response mediators (n-6 polyunsaturated fatty acids, such as AA and linoleic acid) and immune response antagonist (n-3 polyunsaturated fatty acids, such as docosahexaenoic acid and docosapentaenoic acid) at 14 dpi. We also found that at 21 dpi the immune response mediators, including one upregulated n-6 polyunsaturated fatty acids (AA), two upregulated saturated fatty acids (stearic acid and palmitic acid) and one downregulated n-6 polyunsaturated fatty acid (linoleic acid), were observed in the infected cerebral cortices. Additionally, two inflammatory antagonists, n-3 polyunsaturated fatty acid (docosahexaenoic acid-n3) and monounsaturated fatty acid (oleic acid), were upregulated. Furthermore, both oleic acid (inflammatory antagonist) and AA (immune response mediator) were identified as *T. gondii* responsive metabolites in the mouse cerebral cortex. These differential changes in the metabolites involved in the biosynthesis of unsaturated fatty acids in the cerebral cortex during *T. gondii* infection (Fig. 4) confirm previous studies [29, 30], suggesting immune-regulatory roles of unsaturated fatty acids during infection with this parasite. Interestingly, all these perturbed fatty acids are products of acyl-CoA thioesterase, indicating that acyl-CoA thioesterases play essential roles in mediating the interaction between *T. gondii* and mouse cerebral cortex.

Downregulated metabolites in cerebral cortex

Out of the 12 pathways that were detected in our study, six included downregulated metabolites at 21 dpi, involved in glycerophospholipid metabolism, choline metabolism in cancer, steroid hormone biosynthesis, AA metabolism, linoleic acid metabolism and steroid biosynthesis. Some of these pathways participate in the regulation of neurological functions such as glycerophospholipid metabolism, steroid hormone biosynthesis and AA metabolism. The notion that *T. gondii* has a significant influence on the host behavior has been widely reported; however, the exact molecular mechanisms that link *T. gondii* infection to behavioral changes remain poorly defined. The membrane of neuronal cell is rich in glycerophospholipid, which is involved in the regulation of several molecular functions, such as generation of second messengers, apoptosis, antioxidant and membrane fusion, and regulation of enzyme activities [37]. Steroid hormone metabolites are barbiturate-like ligands of gamma-aminobutyric acid (GABA) receptor [38], which are expressed on the membrane of neurons and are downregulated by *T. gondii*. Alteration of AA metabolism has been implicated in neurological and psychiatric disorders [39]. In

the present study, 21, 8, 5 and 11 metabolites involved in glycerophospholipid metabolism, steroid hormone biosynthesis, steroid biosynthesis and AA metabolism pathways, respectively, were downregulated at 21 dpi. The downregulation of metabolites in these neural activity-related pathways during latent infection may contribute to host behavioral changes.

It is worth noting that steroid hormone controls cytokine production of several immune cells [40]. Once metabolized by enzymes such as cyclooxygenases (COXs), lipoxygenases (LOs) and cytochrome P450 monooxygenases (CYPs), AA breaks down into several biologically active substances which activate host inflammatory response [41]. Although AA was identified as a *T. gondii* responsive metabolite and was upregulated in the present study, the metabolites of AA metabolism pathway were downregulated. This agrees with previous data showing that the enzymes of AA pathway are downregulated in mouse liver infected with *T. gondii* [42]. Furthermore, although steroid hormone biosynthesis pathway and AA metabolism pathway were upregulated in the murine liver and spleen during chronic *T. gondii*, the AA metabolism pathway was downregulated in the liver of acutely infected mice [18, 19].

In addition to AA, eight other *T. gondii* responsive metabolites were identified, namely galactosylsphingosine, LysoSM(d18:1), L-palmitoylcarnitine, calcitetrol, 27-Deoxy-5b-cyprinol, L-homophenylalanine, oleic acid and ceramide (Fig. 6). The accumulation of galactosylsphingosine (also known as psychosine) can result in oligodendroglial cell death and neural signaling dysfunction [43], which influences an animal's behavior. Galactosylsphingosine was upregulated at 14 and 21 dpi (Additional file 2: Table S1). Whether the upregulation of galactosylsphingosine in mouse cerebral cortex contributes to *T. gondii* influence on mouse behavioral changes remains to be investigated. Calcitetrol (also known as 1,25-dihydroxyvitamin D3) participates in the regulation of T_{reg} cells [44]. Ceramide and oleic acid were upregulated at 21 dpi. Oleic acid (a monounsaturated fatty acid) serves as an inflammatory antagonist. In contrast, ceramide activates NLRP3 inflammasome [45], which is required for the control of *T. gondii* in macrophages [46]. Although functions of 27-Deoxy-5b-cyprinol, L-palmitoylcarnitine and LysoSM(d18:1) in the nervous system or immune system have not been elucidated, they could play as yet unknown roles in mediating the interaction between *T. gondii* and the host cerebral cortex.

Conclusions

To our knowledge, this study provides the first comprehensive characterization of cerebral cortex metabolome following *T. gondii* infection in mice. We identified 73, 67 and 276 differentially abundant metabolites, which were involved in 25, 37 and 64 pathways at 7, 14 and 21 dpi, respectively. Differentially abundant metabolites related to biosynthesis of unsaturated fatty acid pathway increased as the infection advances. Twelve perturbed pathways related to neural activity, such as biosynthesis pathways of steroid hormone and arachidonic acid metabolism, were detected in all cerebral cortices at 7, 14 and 21 dpi. Nine metabolites were identified as responsive to *T. gondii* infection. Further analysis of these metabolites will enable the identification of new factors involved in the pathogenesis of cerebral toxoplasmosis.

Additional files

Additional file 1: Figure S1. Agarose gel electrophoresis of PCR amplicons after amplification of *T. gondii* B1 gene DNA from cerebral cortices of *T. gondii*-infected and uninfected mice. Gels were stained with ethidium bromide and DNA was visualized under UV. *Abbreviations*: M, DL1000 DNA marker (TaKaRa, China); P, positive control; N, negative control.

Additional file 2: Table S1. Differentially expressed metabolites that were mapped to the KEGG pathways.

Abbreviations

AA: arachidonic acid; GLT-1: glutamate transporter 1; LC–MS: liquid chromatography–mass spectrometry; SPF: specific-pathogen-free; PBS: phosphate-buffered saline; QC: quality control; SPE: solid phase extraction; UPLC: ultra-performance liquid chromatography; MS/MS: tandem mass spectrometry; HMDB: The Human Metabolome Database; KEGG: Kyoto Encyclopedia of Genes and Genomes; ESI−: negative electrospray ionization; ESI+: positive electrospray ionization; PLS-DA: partial least squares-discriminant analysis; ROC: receiver operating characteristic; AUC: area under the curve; GPI: glycosylphosphatidylinositol.

Acknowledgements

The authors are thankful for the technical assistance provided by BGI-Shenzhen, China.

Authors' contributions

HME and XQZ conceived and designed the study and critically revised the manuscript. JM performed the experiment, analyzed the metabolomics data and drafted the manuscript. JJH and CXZ helped in data analysis and manuscript revision. JLH and FKZ helped in study implementation. All authors read and approved the final manuscript.

Funding

This work received financial support from the International Science and Technology Cooperation Project of Gansu Provincial Key Research and Development Program (Grant No. 17JR7WA031), the Elite Program of Chinese Academy of Agricultural Sciences, and the Agricultural Science and Technology Innovation Program (ASTIP) (Grant No. CAAS-ASTIP-2016-LVRI-03).

Availability of data and materials

The datasets supporting the findings of this article are included within the paper. The metabolomics data have been deposited in the MetaboLights

database (http://www.ebi.ac.uk/metabolights) with accession number MTBLS770.

Ethics approval and consent to participate
All mice were handled strictly in accordance with the Animal Ethics Procedures and Guidelines of the People's Republic of China. The study protocol was reviewed and approved by the Animal Administration and Ethics Committee of Lanzhou Veterinary Study Institute, Chinese Academy of Agricultural Sciences.

Consent for publication
Not applicable.

Competing interests
The authors declare that they have no competing interests.

Author details
[1] State Key Laboratory of Veterinary Etiological Biology, Key Laboratory of Veterinary Parasitology of Gansu Province, Lanzhou Veterinary Research Institute, Chinese Academy of Agricultural Sciences, Lanzhou 730046, Gansu, People's Republic of China. [2] Department of Parasitology, Shandong University School of Basic Medicine, Jinan 250012, Shandong, People's Republic of China. [3] Faculty of Medicine and Health Sciences, School of Veterinary Medicine and Science, University of Nottingham, Sutton Bonington Campus, Loughborough LE12 5RD, UK.

Received: 22 March 2019 Accepted: 19 July 2019
Published online: 29 July 2019

References

1. Pappas G, Roussos N, Falagas ME. Toxoplasmosis snapshots: global status of *Toxoplasma gondii* seroprevalence and implications for pregnancy and congenital toxoplasmosis. Int J Parasitol. 2009;39:1385–94.
2. Ustun S, Aksoy U, Dagci H, Ersoz G. Incidence of toxoplasmosis in patients with cirrhosis. World J Gastroenterol. 2004;10:452–4.
3. Shapira Y, Agmon-Levin N, Renaudineau Y, Porat-Katz BS, Barzilai O, Ram M, et al. Serum markers of infections in patients with primary biliary cirrhosis: evidence of infection burden. Exp Mol Pathol. 2012;93:386–90.
4. Jones-Brando L, Torrey EF, Yolken R. Drugs used in the treatment of schizophrenia and bipolar disorder inhibit the replication of *Toxoplasma gondii*. Schizophr Res. 2003;62:237–44.
5. Brooks JM, Carrillo GL, Su J, Lindsay DS, Fox MA, Blader IJ. *Toxoplasma gondii* infections alter GABAergic synapses and signaling in the central nervous system. MBio. 2015;6:e01428–515.
6. Ingram WM, Goodrich LM, Robey EA, Eisen MB. Mice infected with low-virulence strains of *Toxoplasma gondii* lose their innate aversion to cat urine, even after extensive parasite clearance. PLoS ONE. 2013;8:e75246.
7. Evans AK, Strassmann PS, Lee IP, Sapolsky RM. Patterns of *Toxoplasma gondii* cyst distribution in the forebrain associate with individual variation in predator odor avoidance and anxiety-related behavior in male Long-Evans rats. Brain Behav Immun. 2014;37:122–33.
8. David CN, Frias ES, Szu JI, Vieira PA, Hubbard JA, Lovelace J, et al. GLT-1-dependent disruption of CNS glutamate homeostasis and neuronal function by the protozoan parasite *Toxoplasma gondii*. PLoS Pathog. 2016;12:e1005643.
9. Gaskell EA, Smith JE, Pinney JW, Westhead DR, McConkey GA. A unique dual activity amino acid hydroxylase in *Toxoplasma gondii*. PLoS ONE. 2009;4:e4801.
10. Notarangelo FM, Wilson EH, Horning KJ, Thomas MA, Harris TH, Fang Q, et al. Evaluation of kynurenine pathway metabolism in *Toxoplasma gondii*-infected mice: implications for schizophrenia. Schizophr Res. 2014;152:261–7.
11. Okusaga O, Duncan E, Langenberg P, Brundin L, Fuchs D, Groer MW, et al. Combined *Toxoplasma gondii* seropositivity and high blood kynurenine—linked with nonfatal suicidal self-directed violence in patients with schizophrenia. J Psychiatr Res. 2016;72:74–81.
12. Jia B, Lu H, Liu Q, Yin J, Jiang N, Chen Q. Genome-wide comparative analysis revealed significant transcriptome changes in mice after *Toxoplasma gondii* infection. Parasit Vectors. 2013;6:161.
13. Tanaka S, Nishimura M, Ihara F, Yamagishi J, Suzuki Y, Nishikawa Y. Transcriptome analysis of mouse brain infected with *Toxoplasma gondii*. Infect Immun. 2013;81:3609–19.
14. Radke J, Worth D, Hong D, Huang S, Sullivan WJ, Wilson E, et al. Transcriptional repression by ApiAP2 factors is central to chronic toxoplasmosis. PLoS Pathog. 2018;14:e1007035.
15. Yang J, Du F, Zhou X-L, Wang L-X, Li S-Y, Fang R, et al. Brain proteomic differences between wild-type and CD44— mice induced by chronic *Toxoplasma gondii* infection. Parasitol Res. 2018;117:2623–33.
16. Sahu A, Kumar S, Sreenivasamurthy SK, Selvan LD, Madugundu AK, Yelamanchi SD, et al. Host response profile of human brain proteome in toxoplasma encephalitis co-infected with HIV. Clin Proteomics. 2014;11:39.
17. Lv L, Wang Y, Feng W, Hernandez JA, Huang W, Zheng Y, et al. iTRAQ-based differential proteomic analysis in *Mongolian gerbil* brains chronically infected with *Toxoplasma gondii*. J Proteomics. 2017;160:74–83.
18. Chen XQ, Elsheikha HM, Hu RS, Hu GX, Guo SL, Zhou CX, et al. Hepatic metabolomics investigation in acute and chronic murine toxoplasmosis. Front Cell Infect Microbiol. 2018;8:189.
19. Chen XQ, Zhou CX, Elsheikha HM, He S, Hu GX, Zhu XQ. Profiling of the perturbed metabolomic state of mouse spleen during acute and chronic toxoplasmosis. Parasit Vectors. 2017;10:339.
20. Zhou CX, Zhou DH, Elsheikha HM, Zhao Y, Suo X, Zhu XQ. Metabolomic profiling of mice serum during toxoplasmosis progression using liquid chromatography–mass spectrometry. Sci Rep. 2016;6:19557.
21. Zhou CX, Zhou DH, Elsheikha HM, Liu GX, Suo X, Zhu XQ. Global metabolomic profiling of mice brains following experimental infection with the cyst-forming *Toxoplasma gondii*. PLoS ONE. 2015;10:e0139635.
22. Berenreiterova M, Flegr J, Kubena AA, Nemec P. The distribution of *Toxoplasma gondii* cysts in the brain of a mouse with latent toxoplasmosis: implications for the behavioral manipulation hypothesis. PLoS ONE. 2011;6:e28925.
23. Dubey JP, Ferreira LR, Alsaad M, Verma SK, Alves DA, Holland GN, et al. Experimental toxoplasmosis in rats induced orally with eleven strains of *Toxoplasma gondii* of seven genotypes: tissue tropism, tissue cyst size, neural lesions, tissue cyst rupture without reactivation, and ocular lesions. PLoS ONE. 2016;11:e0156255.
24. Elsheikha HM, Busselberg D, Zhu XQ. The known and missing links between *Toxoplasma gondii* and schizophrenia. Metab Brain Dis. 2016;31:749–59.
25. Ihara F, Nishimura M, Muroi Y, Mahmoud ME, Yokoyama N, Nagamune K, et al. *Toxoplasma gondii* infection in mice impairs long-term fear memory consolidation through dysfunction of the cortex and amygdala. Infect Immun. 2016;84:2861–70.
26. Martins-Duarte ES, Carias M, Vommaro R, Surolia N, de Souza W. Apicoplast fatty acid synthesis is essential for pellicle formation at the end of cytokinesis in *Toxoplasma gondii*. J Cell Sci. 2016;129:3320–31.
27. Ramakrishnan S, Docampo MD, Macrae JI, Pujol FM, Brooks CF, van Dooren GG, et al. Apicoplast and endoplasmic reticulum cooperate in fatty acid biosynthesis in apicomplexan parasite *Toxoplasma gondii*. J Biol Chem. 2012;287:4957–71.
28. Pernas L, Bean C, Boothroyd JC, Scorrano L. Mitochondria restrict growth of the intracellular parasite *Toxoplasma gondii* by limiting its uptake of fatty acids. Cell Metab. 2018;27(886–97):e4.
29. Grimble RF, Tappia PS. Modulation of pro-inflammatory cytokine biology by unsaturated fatty acids. Z Ernahrungswiss. 1998;37(Suppl. 1):57–65.
30. Milanski M, Degasperi G, Coope A, Morari J, Denis R, Cintra DE, et al. Saturated fatty acids produce an inflammatory response predominantly through the activation of TLR4 signaling in hypothalamus: implications for the pathogenesis of obesity. J Neurosci. 2009;29:359–70.
31. Langenbach R, Morham SG, Tiano HF, Loftin CD, Ghanayem BI, Chulada PC, et al. Prostaglandin synthase 1 gene disruption in mice reduces arachidonic acid-induced inflammation and indomethacin-induced gastric ulceration. Cell. 1995;83:483–92.
32. O'Shea M, Bassaganya-Riera J, Mohede IC. Immunomodulatory properties of conjugated linoleic acid. Am J Clin Nutr. 2004;79:1199S–206S.

33. Schaeffler A, Gross P, Buettner R, Bollheimer C, Buechler C, Neumeier M, et al. Fatty acid-induced induction of Toll-like receptor-4/nuclear factor-kappaB pathway in adipocytes links nutritional signalling with innate immunity. Immunology. 2009;126:233–45.
34. Weldon SM, Mullen AC, Loscher CE, Hurley LA, Roche HM. Docosahexaenoic acid induces an anti-inflammatory profile in lipopolysaccharide-stimulated human THP-1 macrophages more effectively than eicosapentaenoic acid. J Nutr Biochem. 2007;18:250–8.
35. Nauroth JM, Liu YC, Van Elswyk M, Bell R, Hall EB, Chung G, et al. Docosahexaenoic acid (DHA) and docosapentaenoic acid (DPAn-6) algal oils reduce inflammatory mediators in human peripheral mononuclear cells in vitro and paw edema *in vivo*. Lipids. 2010;45:375–84.
36. Jeffery NM, Yaqoob P, Newsholme EA, Calder PC. The effects of olive oil upon rat serum lipid levels and lymphocyte functions appear to be due to oleic acid. Ann Nutr Metab. 1996;40:71–80.
37. Farooqui AA, Horrocks LA, Farooqui T. Glycerophospholipids in brain: their metabolism, incorporation into membranes, functions, and involvement in neurological disorders. Chem Phys Lipids. 2000;106:1–29.
38. Majewska MD, Harrison NL, Schwartz RD, Barker JL, Paul SM. Steroid hormone metabolites are barbiturate-like modulators of the GABA receptor. Science. 1986;232:1004–7.
39. Bosetti F. Arachidonic acid metabolism in brain physiology and pathology: lessons from genetically altered mouse models. J Neurochem. 2007;102:577–86.
40. Daynes RA, Araneo BA, Hennebold J, Enioutina E, Mu HH. Steroids as regulators of the mammalian immune response. J Invest Dermatol. 1995;105(1 Suppl):14S–9S.
41. Levick SP, Loch DC, Taylor SM, Janicki JS. Arachidonic acid metabolism as a potential mediator of cardiac fibrosis associated with inflammation. J Immunol. 2007;178:641–6.
42. He JJ, Ma J, Elsheikha HM, Song HQ, Huang SY, Zhu XQ. Transcriptomic analysis of mouse liver reveals a potential hepato-enteric pathogenic mechanism in acute *Toxoplasma gondii* infection. Parasit Vectors. 2016;9:427.
43. Hawkins-Salsbury JA, Parameswar AR, Jiang X, Schlesinger PH, Bongarzone E, Ory DS, et al. Psychosine, the cytotoxic sphingolipid that accumulates in globoid cell leukodystrophy, alters membrane architecture. J Lipid Res. 2013;54:3303–11.
44. Xie Z, Chen J, Zheng C, Wu J, Cheng Y, Zhu S, et al. 1,25-dihydroxyvitamin D3 -induced dendritic cells suppress experimental autoimmune encephalomyelitis by increasing proportions of the regulatory lymphocytes and reducing T helper type 1 and type 17 cells. Immunology. 2017;152:414–24.
45. Scheiblich H, Schlutter A, Golenbock DT, Latz E, Martinez-Martinez P, Heneka MT. Activation of the NLRP3 inflammasome in microglia: the role of ceramide. J Neurochem. 2017;143:534–50.
46. Moreira-Souza ACA, Almeida-da-Silva CLC, Rangel TP, Rocha GDC, Bellio M, Zamboni DS, et al. The P2X7 receptor mediates *Toxoplasma gondii* control in macrophages through canonical NLRP3 inflammasome activation and reactive oxygen species production. Front Immunol. 2017;8:1257.

Publisher's Note